



Orbital Debris

Quarterly News

Volume 25, Issue 2
June 2021

Inside...

Nick Johnson,
Former NASA Chief
Scientist Passes..... 3

Goldstone OD Radar:
Historical Review
from a Decade of
Observations
(2007-2017)..... 3

DebrisSat Project
Status Update..... 7

Meeting Report..... 10

Upcoming
Meetings..... 11

Space Missions
and Satellite
Box Score..... 12



A publication of the
NASA Orbital Debris
Program Office (ODPO)

Two On-Orbit Breakup Events in March

The 18th Space Control Squadron (18 SPCS) of the U.S. Space Force detected the first two on-orbit breakup events of 2021 in March. The first breakup was associated with NOAA 17 (International Designator 2002-032A, Catalog number 27453) on 10 March at approximately 7:11 GMT and the second breakup was associated with YunHai 1-02 (International Designator 2019-063A, Catalog number 44547) on 18 March at approximately 7:41 GMT.

The U.S. NOAA 17 meteorological satellite, shown stowed for launch in Figure 1, was launched in 2002. It successfully completed its mission and was decommissioned in 2013. Prior to the breakup, the 1457 kg spacecraft was on an 817 x 800 km altitude orbit with an inclination of 98.62°.

As of 22 April, 102 fragments have been identified and tracked by the 18 SPCS. The Gabbard diagram for this breakup is shown in Figure 2. A similar decommissioned spacecraft, NOAA 16, also experienced a breakup in 2015 (ODQN, vol. 20, issue 1&2, p. 1).

China's YunHai 1-02, also a meteorological satellite, was launched in September 2019. It is likely that YunHai 1-02 still was operational when the breakup occurred. The orbit of the spacecraft prior to the breakup was 785 x 780 km altitude with an inclination of 98.54°. As of 22 April, 43 fragments from the breakup of YunHai 1-02 have been identified and tracked by the 18 SPCS. The Gabbard diagram for this breakup is shown in Figure 3. ♦

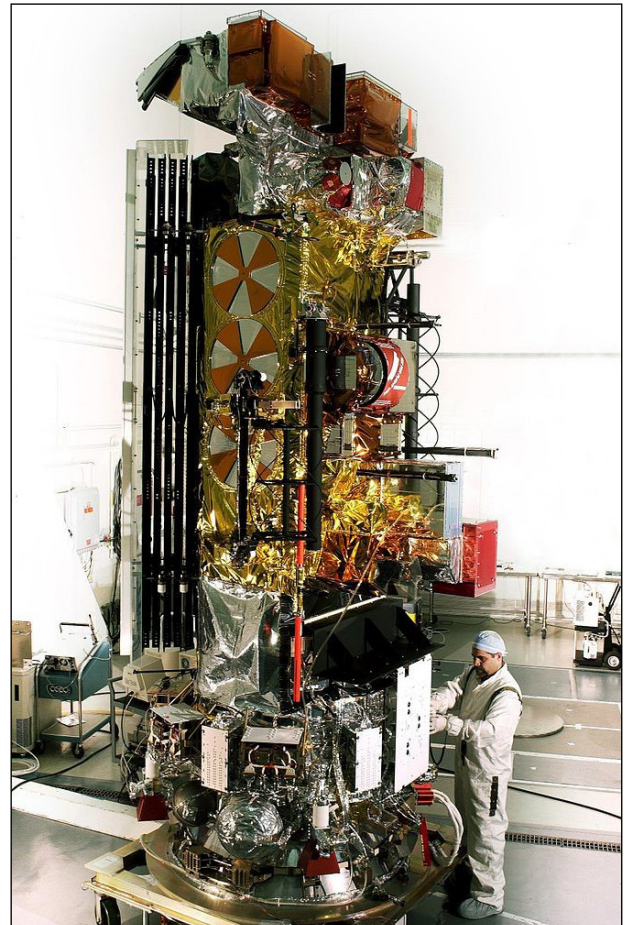


Figure 1. NOAA-17 before launch. Source: NOAA Photo Library, courtesy of NASA (https://en.wikipedia.org/wiki/NOAA-17#/media/File:NOAA-M_before_launch.jpg).

continued on page 2

Breakups

continued from page 1

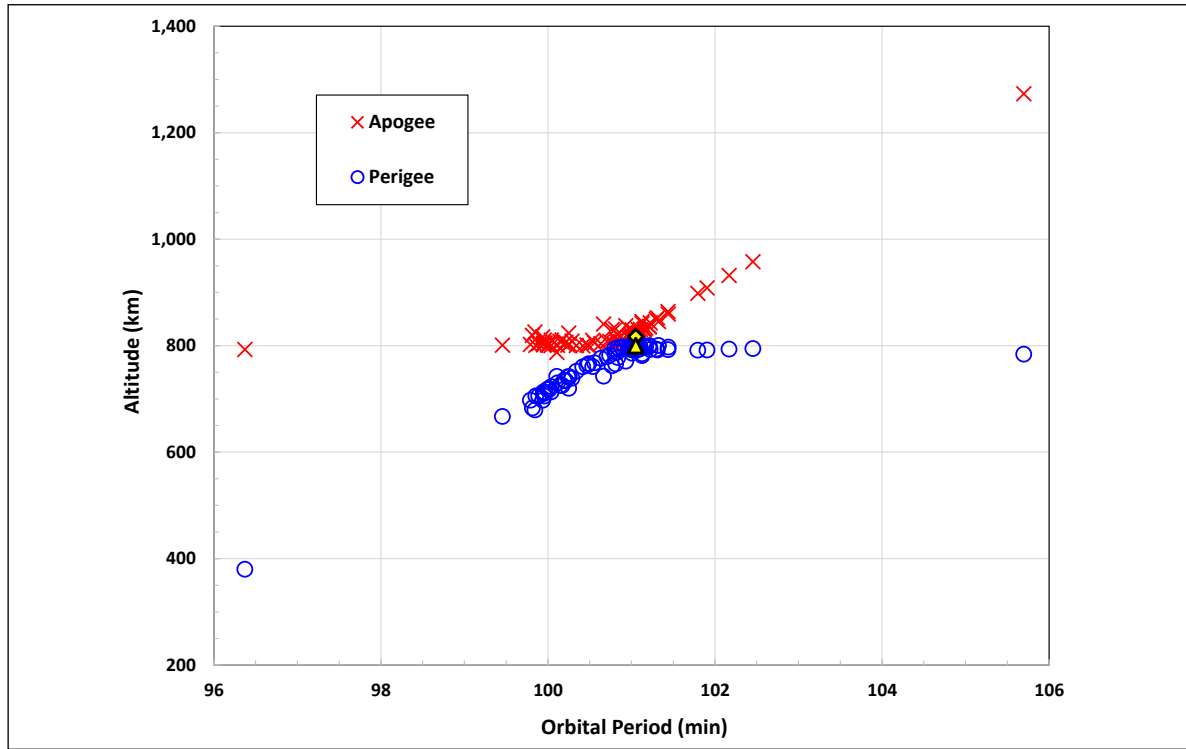


Figure 2. Gabbard diagram of the NOAA 17 breakup fragments. Approximate epoch is early April 2021. The apogee (yellow-filled black diamond) and perigee (yellow-filled black triangle) altitudes of the parent object, NOAA 17, are also shown.

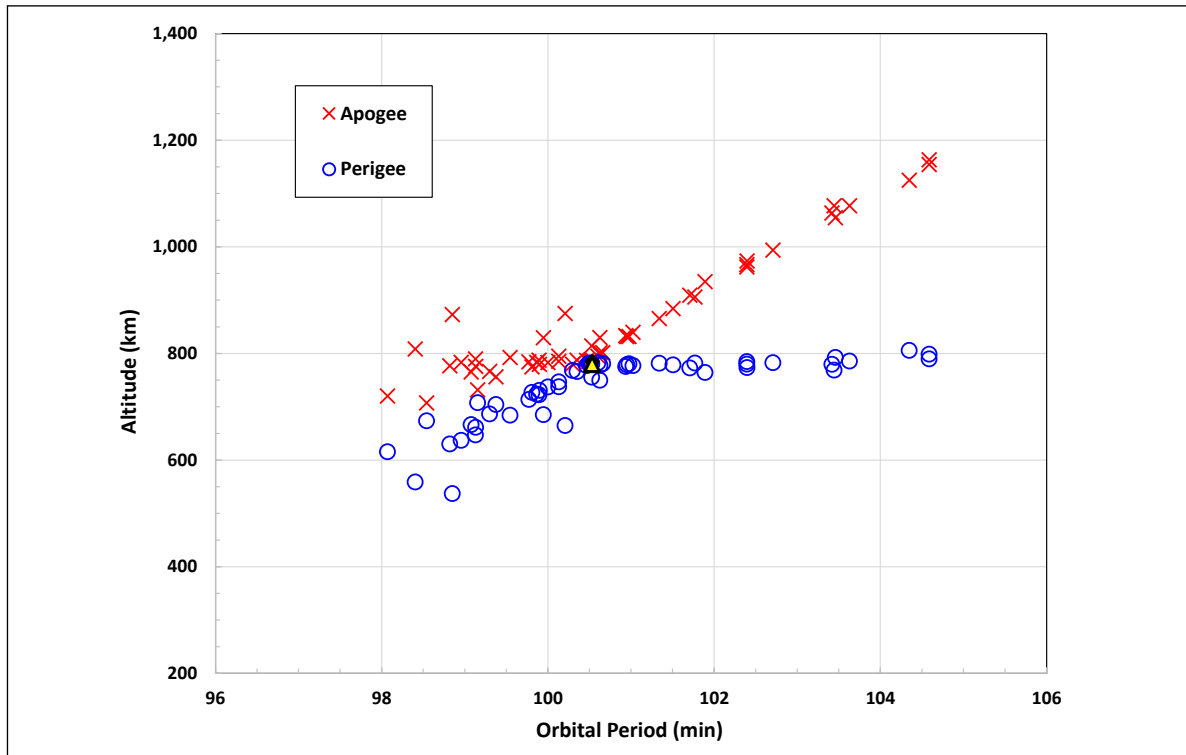


Figure 3. Gabbard diagram of the YunHai 1-02 breakup fragments. Approximate epoch is early April 2021. The apogee (yellow-filled black diamond) and perigee (yellow-filled black triangle) altitudes of the parent object, YunHai 1-02, are also shown. Note the apogee and perigee points are coincident in this plot.

Nick Johnson, Former NASA Chief Scientist for Orbital Debris Passes



Mr. Nicholas Johnson, NASA Chief Scientist for Orbital Debris from 1996 to 2014, passed away on 12 April, 2021. As the NASA Chief Scientist for Orbital Debris, Mr. Johnson served as the agency authority for orbital debris, including all aspects of environment definition, present and future, and the operational and design implications of the environment to human spaceflight and robotic missions operating in Earth orbit. He was responsible for conceiving, conducting, and directing

research to define the orbital debris environment, for determining operational techniques for spacecraft to protect themselves from debris impacts, and for recommending techniques to minimize the growth in the future orbital debris environment.

During his early career, Mr. Johnson served in the Air Force as an aviation electronics technician and had one tour of duty in Vietnam. Later, as an officer in the U.S. Navy, Mr. Johnson was an instructor and served as Director of the Heat Transfer and Fluid Flow Division at the Navy's Nuclear Power School.

Mr. Johnson worked in industry from 1979 to 1996, first at Teledyne Brown Engineering and later at Kaman Sciences. He was an expert on space surveillance and the Soviet space program. He also worked on the Strategic Defense Initiative and the F-15 Anti-Satellite (ASAT) missile program. From these experiences, he became a strong advocate for limiting the generation of orbital debris.

After joining NASA, Mr. Johnson worked diligently to broaden and strengthen orbital debris mitigation guidelines and standards within NASA, the U.S. Government, and internationally. Due to Mr. Johnson's leadership, the U.S. Government Orbital Debris Mitigation Standard Practices were established in 2001 and the United Nations (UN) Committee on the Peaceful Uses of Outer Space (COPUOS) Space Debris Mitigation Guidelines were endorsed by the UN General Assembly in 2007. Mr. Johnson also led the U.S. delegation to the Inter-Agency Space Debris Coordination Committee from 1996 to 2013.

Mr. Johnson is the author of 18 books and more than 200 papers. He has received many awards, including the NASA Distinguished Service Medal, the NASA Exceptional Achievement Medal, the Astronaut Corps Silver Snoopy Award, the Department of Defense's Joint Meritorious Civilian Service Award, the Joseph P. Loftus Space Sustainability Award from the International Association for the Advancement of Space Safety, and the Russian Order of Gagarin.

In 2014, Mr. Johnson retired from NASA. His many technical accomplishments and contributions to the orbital debris community will be sorely missed. ♦

PROJECT REVIEW

Goldstone Orbital Debris Radar: A Historical Review from a Decade of Observations (2007-2017)

R. MILLER, J. MURRAY, AND T. KENNEDY

The NASA Orbital Debris Program Office (ODPO) has utilized the NASA Goldstone bistatic radar since the early 1990's to statistically characterize the low Earth orbit (LEO) sub-centimeter orbital debris (OD) population. Due to the limited number of hours that are available from this radar each year, it is often used to validate measurements obtained by other radar data sources in the range of orbital debris sizes where the radar systems have an overlap. The Goldstone radar provides significantly better sensitivity than is available from other ground-based radar data sources, enabling it to

observe smaller-sized populations of orbital debris. The radar provides a unique capability to detect orbital debris population sizes down to an approximate size of 3 mm for altitudes less than 1000 km. This is important since millimeter-sized orbital debris drives mission-ending risk to robotic spacecraft in LEO. The size discussed is not a directly observed parameter from the radar system, but rather a derived parameter known as characteristic length that is translated from radar cross section (RCS) via the NASA size estimation model (SEM). Over the decade of observations from 2007 to 2017,

continued on page 4

Goldstone 07-17

continued from page 3

significant on-orbit events have occurred including the anti-satellite test against Fengyun 1C and the accidental collision between Cosmos 2251 and Iridium 33. The orbital debris flux is reviewed in this article for several key altitude regimes in LEO.

The Goldstone radar is part of the larger Goldstone Deep Space Communications Complex, which is itself a part of the NASA Deep Space Network operated by the Jet Propulsion Laboratory (JPL). The Goldstone orbital debris data collected between 2007 and 2017 used Deep Space Sensors (DSS) 14 (70 m-diameter antenna) and 15 (34 m-diameter antenna) in bistatic mode. This bistatic radar baseline is approximately 500 m. Goldstone operates in a beam park mode, where the transmitter, DSS-14, is pointed at 75° elevation from the

horizon and 90° azimuth (due east). This pointing is referred to as 75E. The receiver is aimed a fraction of a degree above 75° elevation and at less than half of a degree north of due east (effectively 89.8° azimuth) to intersect the boresight of DSS-14 at a slant range of 550 km. This pointing enables the 3 dB beam overlap of both beams to cover slant ranges starting at 374 km through 3373 km, or approximately 356 km to 3291 km in altitude.

A summary of the hours for orbital debris data collection on an annual basis from 2007 to 2017 are presented in Table 1. Also shown in Table 1 are the total number of orbital debris detections observed in each year for the 75E pointing, the average detection count-rate from each year, and the SEM size at which the collection is considered

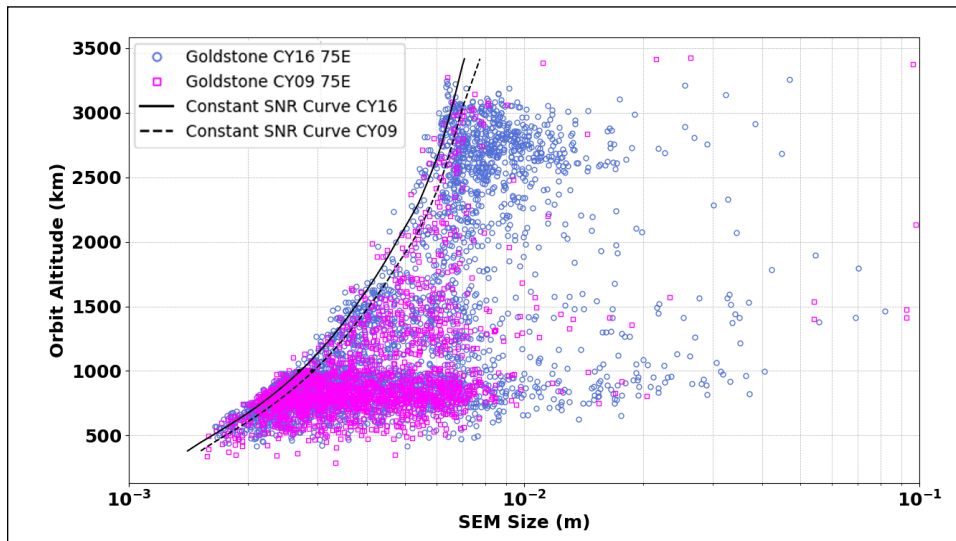


Figure 1. Orbit altitude versus SEM size for Goldstone CY2009 and CY2016 data, with constant signal-to-noise ratio (SNR) curves developed for an object having the completeness size at 1000 km – shown in dashed and solid black lines respectively.

complete at 1000 km altitude - this may also be referred to as completeness size. This is computed empirically for each data set by determining at what point the cumulative RCS curve begins to “roll over” from a power-law distribution due to the drop in the detection probability. There are still detections below this threshold, though the lower detection rate means these counts will be incomplete. A more in-depth review of the process by which these sizes were estimated can be found in [1]. Analysis by ODPO of the Goldstone data in 2014 indicated anomalies in the data collected, which continues to be investigated by JPL and ODPO to determine if the issue is correctable. As a result, data from 2014 is not included in further analysis in this article. A 2017 issue with the transmitter resulted in a reduction in sensitivity in the latter half of 2017. The “2017 A” dataset is data collected prior to 16 September 2017 and the “2017

Table 1. Goldstone CY2007–2017 Data Collection Summary of the Curated Dataset.

Calendar Year (CY)	Total Hours Observed (hrs)	Total Number of Valid Detections	Average Count Rate (hr ⁻¹)	Completeness Size (mm) at 1000 km
2007	6.3	136	21.7	3.4
2008	97.5	3075	31.5	2.9
2009	36.2	1656	45.8	2.9
2010	10.9	379	34.9	3
2011	63.2	3059	48.4	2.7
2012	88.7	4295	48.4	2.6
2013	72.0	3918	54.4	2.7
2014	117.4	3970	33.8	2.7
2015	99.4	5281	53.6	2.5
2016	45.2	3343	74.0	2.7
2017 A	38.2	2234	58.6	3
2017 B	13.7	754	55.4	3.1
Totals	688.6	32100		

continued on page 5

Goldstone 07-17

continued from page 4

Bⁿ dataset is the data collected afterwards. Additionally, analysis of 2017 A showed an anomalously low sodium potassium (NaK) count rate and as a result, it was separated from the analysis in the report. Further analysis of the calendar year (CY)2017 datasets can be found in [1].

Several upgrades were incorporated throughout the years considered in this article, which generally improved the sensitivity of the radar over time. In 2011, a wideband system upgrade resulted in higher sensitivity, lowering the completeness size. Four years later, improvements were integrated to lower the overall system noise temperature, which further decreased the completeness size, as shown in Table 1 for CY2015.

To illustrate the effects of the sensitivity improvements over time, Figure 1 includes constant signal-to-noise ratio (SNR) curves plotted over the orbit altitude versus NASA SEM size for CY2009 and CY2016. The SNR is determined from an object having the completeness size at an altitude of 1000 km. Note that the improved sensitivity in CY2016 relative to CY2009 results in the constant SNR curve shifting towards smaller SEM sizes at a given altitude.

An overall understanding of the OD environment can be obtained by monitoring the debris flux. The surface area flux values reported are the cumulative counts for a given SEM size and larger for a given altitude band, divided by the lateral surface area of the 3 dB beamwidth of the radar, divided by the total observation time for a particular year. The evolution of the OD environment for SEM sizes 3.2 mm and larger within the 800 km to 850 km altitude band over the time of observations is shown in Figure 2. The 800 km to 850 km altitude band was chosen due to it having a relatively large OD flux compared to other LEO altitudes, as well as hosting the NOAA polar orbiting weather spacecraft constellation. There is an increase in the flux observed in this altitude band during 2007–2017, with a significant jump observed in this SEM size flux in 2009. This increase in 2009 is likely a result of the Iridium 33 and Cosmos 2251 collision that occurred on 10 February 2009. For 2011 and several years after, the flux appears to have stabilized, with slight increases being observed in 2016 and 2017. It should be noted that the Goldstone 75E pointing started in December 2007, and observations prior to the Fengyun-1C antisatellite test in January 2007 for this pointing are unavailable.

A similar review of the flux for the SEM size 3.2 mm and larger OD population in the 400 km to 450 km altitude band is shown in Figure 3; this band contains the nominal orbit altitude for the International Space Station. In general, the counting statistics are not as accurate in this altitude regime as at higher altitudes since there are simply fewer objects and a narrower beam, as well as a relatively small number of observation hours available from Goldstone. Although the uncertainties are larger, there is still some evidence of a flux increase from 2009 to 2010. This may be due to the events in 2009.

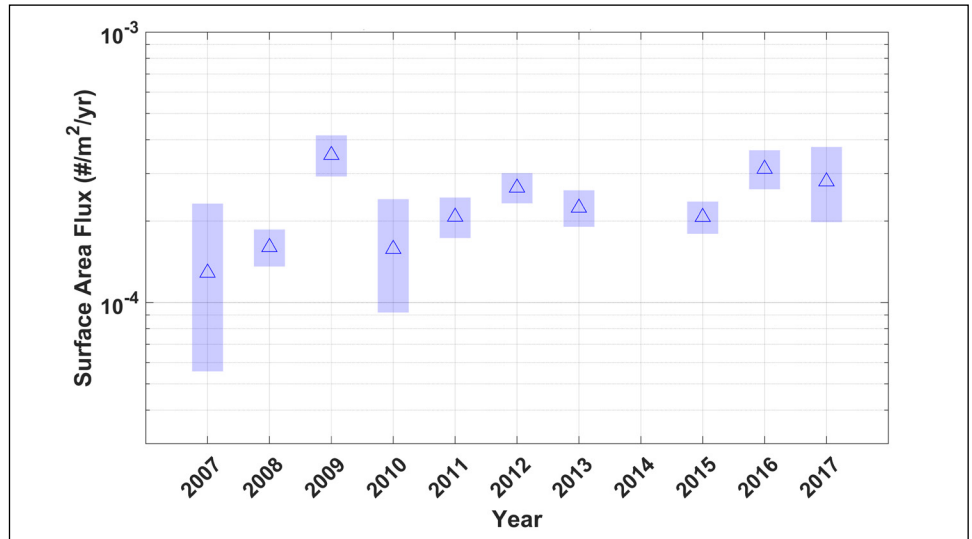


Figure 2. Plot of the evolution of surface area flux for Goldstone CY2007–CY2017, for SEM size greater than or equal to 3.2 mm and between 800 km and 850 km altitudes. The triangles represent the measured surface area flux and the shaded regions represent the two- σ Poisson uncertainty bounds.

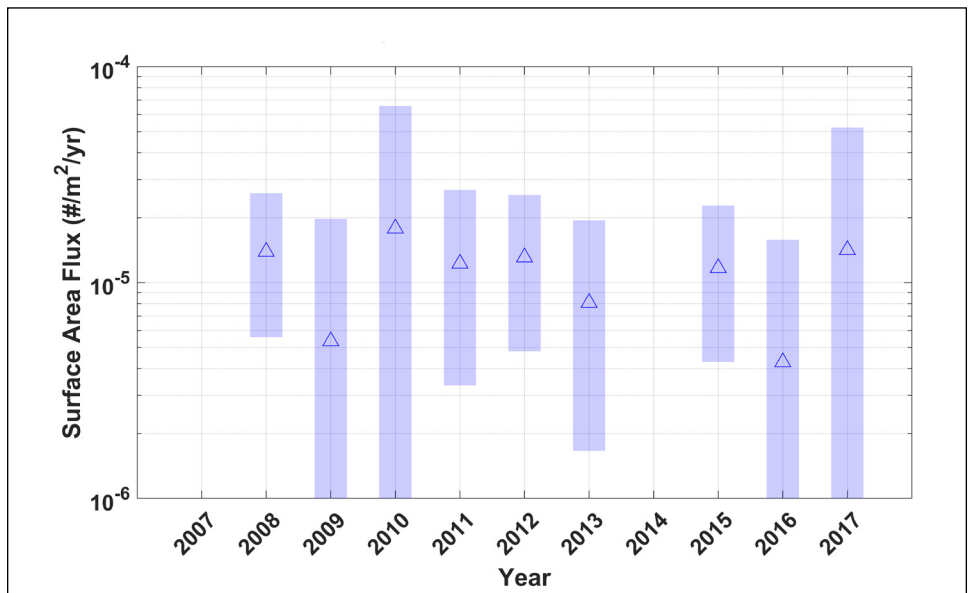


Figure 3. Plot of the evolution of surface area flux for Goldstone CY2007–CY2017, for SEM size greater than or equal to 3.2 mm and between 400 km and 450 km altitudes. The shaded regions represent the two- σ Poisson uncertainty bounds.

continued on page 6

Goldstone 07-17

continued from page 5

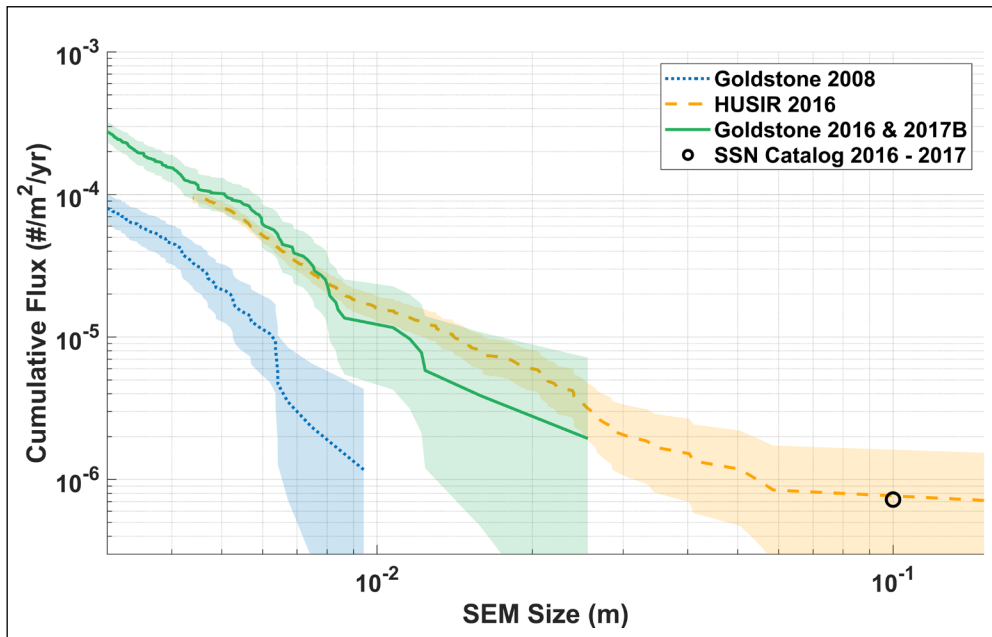


Figure 4. Comparison of the surface area flux vs SEM size between different observation years at Goldstone, HUSIR, and the SSN catalog. Shaded regions represent the two- σ Poisson uncertainty bounds.

From 2011 and later, the flux appears to be relatively stable, aside from a possible drop in the observed flux in 2016. Due to the low number of hours for the Goldstone 75E pointing, as well as the typically sparse counts in the 400 km to 450 km altitude region, there were no OD observations with SEM sizes > 3.2 mm in this altitude band for 2007.

In addition to summarizing the flux to a limiting size in several key altitude regimes, it is of interest to review the SEM size distribution of orbital debris in the important 700 km to 750 km altitude region. The 700 km to 750 km altitude band contains the nominal orbit altitudes of A-Train Earth-observing satellite constellation. In Figure 4, the cumulative flux as a function of SEM size in this altitude band is presented for three different years (CY2008, CY2016, and CY2017 B). For comparison, data acquired in 2016 from the Haystack Ultrawideband Satellite Imaging Radar (HUSIR) and cataloged data from 2016-2017 (down to a completeness of 10 cm in LEO) is shown. The Space Surveillance Network (SSN) catalog data point is the flux that the radar is expected to observe based on the SSN catalog population, sampling the SSN catalog from day of year (DOY) 180 in 2016 through DOY 180 in 2017. Goldstone data from 2016 and 2017 B are combined in Figure 4 due to the relatively small number

of hours in the 2017 B dataset, as well as the larger number of observation hours collected in 2008.

For SEM sizes larger than 1 cm, Goldstone data typically is not used since the radar is believed to saturate with OD objects larger than this size. HUSIR data is referenced to (a) demonstrate consistency of HUSIR and Goldstone data in their size overlap region and (b) show the overall SEM size distribution as it transitions from the detection limit of the SSN catalog to SEM sizes where Goldstone data becomes reliable. The HUSIR and Goldstone data in 2016 and 2017 agree relatively well in the region of overlap between SEM sizes of 1 cm and the HUSIR limiting size of about 5.5 mm. For smaller SEM-sized OD objects, Goldstone data is used to its limiting size threshold of about 3 mm, depending upon observation year. Note that the cumulative flux for Goldstone observations in the later years shows a significant increase in flux relative to 2008. This is likely due to several

on-orbit fragmentation events, the most prominent of which is the Cosmos-2251/Iridium-33 collision.

This article has described Goldstone radar observations of the OD environment in LEO from 2007 to 2017. Analysis of the evolution of the smaller-sized OD objects that can be detected in several prioritized altitude regimes and their estimated completeness has been described. An important finding is the increased OD flux observed in each of these altitudes in the later years relative to the start of the survey. Flux measurements made between 2011 and 2017 appear to be relatively stable and consistent with HUSIR radar observations down to HUSIR's limiting size.

These results are expected to provide a valuable reference for ODPO models, such as the Orbital Debris Engineering Model (ORDEM) 4.0, due to the uniqueness of Goldstone radar observations at sizes smaller than can be observed by HUSIR.

Reference

1. Miller, R., *et al.*, "Goldstone Radar Measurements of the Orbital Debris Environment: 2007-2017," NASA Johnson Space Center, Houston, TX, USA. Unpublished manuscript in work. ♦

SUBSCRIBE to the ODN or UPDATE YOUR SUBSCRIPTION ADDRESS

If you would like to be notified when a new issue of the ODN is published or need to update your email address, use the ODN Subscription Request Form located on the NASA Orbital Debris Program Office (ODPO) website at <https://orbitaldebris.jsc.nasa.gov/quarterly-news/>.

To fill out the form, either click on the heading "Subscribe to the Quarterly News," or navigate directly by using the URL: <https://orbitaldebris.jsc.nasa.gov/quarterly-news/subscription.cfm>.

PROJECT REVIEW

DebrisSat Project Status Update

H. COWARDIN, J. MURRAY, A. MANIS, J. OPIELA,
AND J.-C. LIOU

The NASA Orbital Debris Program Office (ODPO) develops, maintains, and updates orbital debris environmental models, such as the NASA Orbital Debris Engineering Model (ORDEM), to support satellite designers and operators by estimating the orbital debris flux on their vehicles in orbit, which can be used for probabilistic risk assessment. Updates to ORDEM utilize the most recent validated datasets from radar, optical, and in situ sources to provide estimates of the debris flux as a function of size, material density, relative velocity, and direction. Efforts are underway to implement a new parameter that can significantly influence the risk – shape. Shape can be related to material density and size to better understand the damage assessments on satellites.

One of the key laboratory tests that is providing insight into shapes and relationships between shape and debris size, mass, and material density, specifically for modern spacecraft, is DebrisSat (ODQN, Vol. 18, Issue 3, pp. 3-5). The DebrisSat project is a collaboration of the ODPO, the U.S. Space Force Space and Missile Systems Center (SMC), The Aerospace Corporation (Aerospace), the University of Florida (UF), and the Air Force Arnold Engineering Development Complex (AEDC). Motivation for the DebrisSat project was based on a key impact test series, the Satellite Orbital Debris Characterization Impact Test (SOCIT), which was conducted by the Department of Defense (DOD) and NASA at the AEDC in 1992 to support the development of satellite breakup models [1].

The main target for SOCIT was a fully functional 1960’s era U.S. Navy Transit satellite. The DOD and NASA breakup models based on the SOCIT data have supported many applications and matched on-orbit events reasonably well over the years [2]. As new materials and construction techniques are developed for modern satellites, there is a need for new laboratory-based tests to acquire data to

improve the existing DOD and NASA breakup models. Thus, the DebrisSat project was developed to conduct a hypervelocity impact test of a high-fidelity satellite mock-up, representative of present-day, low Earth orbit spacecraft, and constructed with modern spacecraft materials and techniques. To increase the project’s benefits further, Aerospace designed and built a target simulating a launch vehicle upper stage (“DebrisLV”) for the pre-test shot. The pre-test shot was conducted two weeks prior to the DebrisSat impact test with identical conditions to DebrisSat (facility set-up, projectile, and impact speed) to guarantee a successful test for the primary target. Table 1 shows a comparison of some SOCIT, DebrisSat, and DebrisLV test conditions.

The DebrisSat project has come a long way since planning efforts initiated in 2009, to successful hypervelocity impact tests of DebrisSat and DebrisLV in 2014, to present day as thorough analyses are being conducted of the fragments generated by the tests. Assessing the material, size, mass, density, and shape distributions for improved characterization of fragmentation events will facilitate updates to ORDEM, existing breakup models used by NASA and the DOD, and will improve the fidelity of orbital debris damage assessments for future missions. The collection, measurement, and characterization of all fragments down to approximately 2 mm in size has continued, and preliminary laboratory measurements are underway to support the development of a new optical Size Estimation Model (SEM), followed by radar facility measurements to support updates to the current radar-based SEM.

All fragments with at least one dimension ≥ 2 mm are carefully collected and/or extracted from the foam panels/pieces that lined the test chamber. The fragments are assigned unique identification numbers before their physical characteristics are determined. During the characterization process, each fragment’s physical (observed and derived) parameters are archived in the DebrisSat Categorization

continued on page 8

Table 1. Experimental details on SOCIT, DebrisSat, and DebrisLV test campaigns

	SOCIT/ Transit	DebrisSat	DebrisLV
Target body dimensions (dia × ht)	46 cm × 30 cm	60 cm × 50 cm	35 cm × 88 cm
Target mass	34.5 kg	56 kg	17.1 kg
Multi-layered Insulation (MLI) and solar panel	No	Yes	No
Projectile material	Al sphere	Hollow Al cylinder with attached nylon bore-rider	Hollow Al cylinder with attached nylon bore-rider
Projectile dimension, mass	4.7 cm diameter, 150 g	8.6 cm × 9 cm, 570 g	8.6 cm × 9 cm, 598 g
Impact speed	6.1 km/sec	6.8 km/sec	6.9 km/sec
Impact Energy to Target Mass ratio (EMR)	81 J/g (2.8 MJ total)	235 J/g (13.2 MJ total)	832 J/g (14.2 MJ total)
Soft-Catch System: Polyurethane foam stacks of three densities	0.06, 0.096, and 0.192 g/cm ³ ; 25 cm thick	0.048, 0.096, and 0.192 g/cm ³ ; up to 61 cm thick	0.048, 0.096, and 0.192 g/cm ³ ; up to 51 cm thick

DebrisSat

continued from page 7

System (DCS). The DCS is a database solution designed and developed specifically to manage the large amount of data generated by the DebrisSat project. The initial characterization step involves assessing

each uniquely identified fragment in terms of material, shape, and color. Mass measurements are acquired using a suite of scales appropriate for the individual fragment's mass. To optimize the characterization

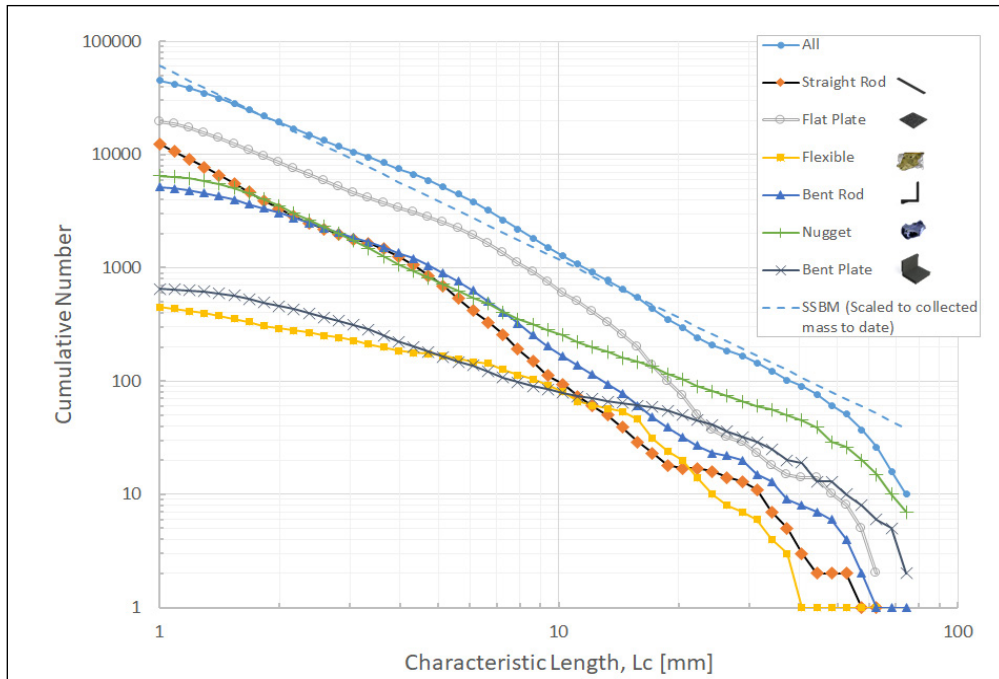


Figure 1. Cumulative number versus L_c as a function of the 6 shape categories used in DebrisSat, as of 14 January 2021.

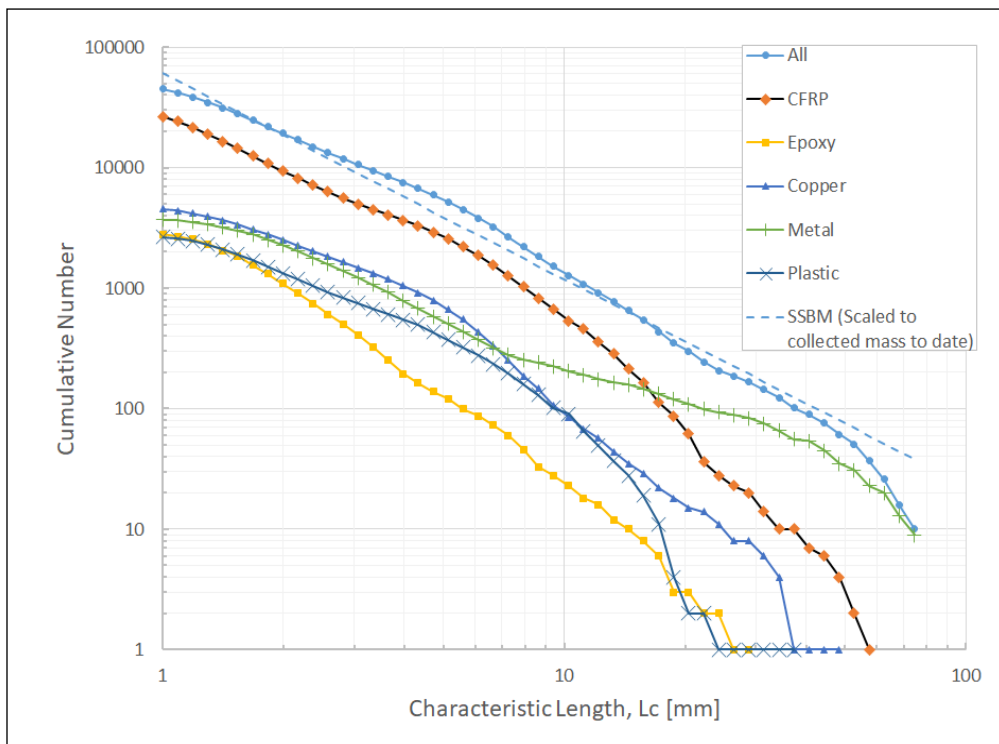


Figure 2. Cumulative number versus L_c as a function of the primary materials in the DebrisSat data, as of 14 January 2021.

process and implement methodologies to minimize biases and/or errors associated with “human-in-the-loop” activities during measurements, 2D and 3D imagers are utilized to measure the physical size based on the solid body dimensions. From these initial measurements, the characteristic length (L_c , defined as the arithmetic average of the object's three maximum orthogonal projected dimensions), average cross-sectional area, volume, and bulk density are calculated and stored in the DCS. Note that the initial set of investigated fragments concentrated on carbon fiber reinforced polymers (CFRP) using the 2D imagers, where the third dimension could be extracted from the material's density. As the project has progressed from these initial homogenous fragments, mirrors have been added to the 2D imaging system to allow measurement of the third dimension. More details on the characterization can be found in [3, 4].

The current NASA Standard Satellite Breakup Model (SSBM) was formulated using laboratory tests, primarily from SOCIT, and ground-based remote measurements of on-orbit fragmentation events to provide an average breakup ensemble for spacecraft and upper stage collisions and explosions. Significant validation efforts against observable data were conducted, including development of the radar SEM, based on radar cross section (RCS) measurements of representative fragments. To determine how to best update or improve future environmental models, such as ORDEM and the SSBM, a statistical assessment must be done to determine the distribution of key parameters (shape, density, and size) using laboratory data. The SSBM uses L_c as the fundamental independent variable in lieu of mass. The choice of L_c in preference to mass was driven by the on-orbit observables, specifically RCS and brightness, which can be directly correlated to size.

More details on the SSBM can be found in [2, 3, 4]. Unlike the SOCIT

continued on page 9

DebriSat

continued from page 8

analysis, which categorized shapes into 10 bins, the DebriSat project focused on 6 specific shape categories with an accompanying rubric used to determine if each fragment is a 1) Flat Plate, 2) Bent Plate, 3) Straight Needle/Rod/Cylinder, 4) Bent Needle/Rod/Cylinder, 5) Parallelepiped/Nugget/Spheroid, or 6) Flexible Shape [3]. In the case of the latter category, Flexible Shape, the shape easily is changed simply through handling so a true shape is not known. Examples of objects in the “Flexible Shape” category include multi-layer insulation (MLI) or a flexible wiring harness used in the construction of DebriSat.

Ongoing analysis of the growing number of fragments as a function of L_c with each database update is shown in Figure 1 and Figure 2. Figure 1 shows the cumulative number of fragments as a function of L_c broken down into the DebriSat fragment shape categories. Additionally, the SSBM prediction for the cumulative number distribution for DebriSat fragments is shown, scaled to the total mass of collected fragments which have a corresponding L_c . Each point on the curves represents the total number of fragments of that size and larger. From 1 mm through 10.74 mm the flat plate category represents the majority of the shape fragments. Based on the current database information, from approximately 2 mm to 3 mm, straight rods, nuggets, and bent rods are equivalently the second most dominant shape category. A transition in shape categories occurs at 3 mm, where bent rods (from 3 mm to 7 mm) and nuggets (from 7 mm to 2 cm) trade off as the second most dominant shape category. After this, nuggets and bent plates, respectively, dominate the larger size regimes. These transitions in shape are associated with the primary materials of the respective shape categories.

In Figure 2, a subset of “All” materials is plotted, specifically the five dominant, primary materials from the database: CFRP, Epoxy, Copper, Metal, and Plastic. Note: the “All” curve in Figure 2 represents all materials currently collected in the database. The CFRP dominates the material category from 1 mm to 16.42 mm. Based on data provided to date, CFRP fragments tend to fall into plate-like or needle-like (straight rod) categories. Therefore, the dominating shapes for fragments near 2 mm and smaller correlates with the dominating CFRP material. At the transition zone of 16.42 mm, the metal category becomes the primary material for larger fragments. Again, the metal fragments tend to fall into nugget-like, plate-like, and bent-plate shape categories consistent with Figure 1.

To further assess the similarities and differences between a modern satellite fragmentation event (DebriSat) and a classic satellite (SOCIT), Figure 3 compares the cumulative number of fragments as a function of L_c for DebriSat and SOCIT. For comparative analysis

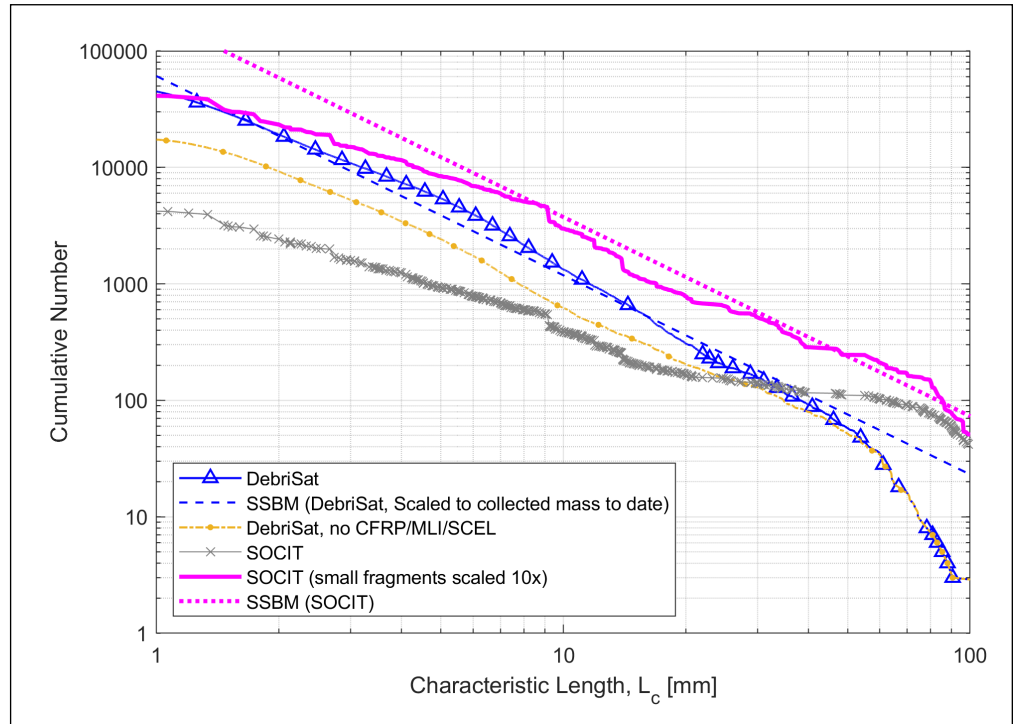


Figure 3. Cumulative number versus L_c for DebriSat (with and without modern materials), SOCIT, and the SSBM for SOCIT and DebriSat (scaled to total mass of collected fragments which have a corresponding L_c), as of 14 January 2021.

purposes, modern materials of CFRP, MLI, and solar cells (SCEL) were also removed from the DebriSat counts to provide a more consistent comparison between the DebriSat and SOCIT datasets. The predicted number of DebriSat fragments as a function of size using the SSBM is also shown, scaled to the total mass of collected fragments which have a corresponding L_c . Note two curves are shown for the SOCIT fragments, including one with small fragments scaled by a factor of 10. This scaling was applied to statistically correct for the fraction of fragments that were collected and analyzed to more accurately represent the likely total fragment distribution [5]. Overall, the slope of the DebriSat fragments matches the SSBM relatively well, both with and without the modern materials. The roll-off at sizes below 2 mm is due to the project limitation of collecting/extracting only fragments with at least one dimension ≥ 2 mm.

The DebriSat project provides the ground-truth data to characterize large and small (millimeter-sized) fragmentation debris. Based on this latest dataset, out of 53,472 fragments measured, nearly 14,000 fragments with a L_c between 2 mm and 5 mm have been characterized. The focus of DebriSat characterization has shifted in recent years to slightly larger size regimes, specifically fragments > 1 cm, to remove any potential biases caused by the dominance of CFRP and to better characterize the distributions as a function of size, shape, material, and material densities. Moving forward, a subset of statistically representative fragments will be analyzed in radar facilities to update the current radar-based SEM, as well as within the ODPO’s Optical Measurement Center located at NASA’s Johnson Space Center to derive an optical SEM. In support of including shape as a new parameter in the next ORDEM development, simulations and tests

continued on page 10

DebrisSat

continued from page 9

are ongoing to characterize impacts from non-spherical projectiles with various densities. These efforts (ODQN, vol 24, Issue 3, pp. 4-7) are being conducted in coordination with the NASA Hypervelocity Impact Technology group to improve damage equations used to assess the vulnerability of spacecraft (or components of spacecraft) due to orbital debris impacts. The ongoing measurement and analytical work resulting from DebrisSat continues to provide critical information for the next-generation models for space object characterization, the orbital debris environment, and risk assessment.

References

1. Krisko, P.H., *et al.*, "SOCIT4 collisional-breakup test data analysis: with shape and material characterization," *Adv. Space Res.* 41(7), pp. 1138-46. (2008).
2. Johnson, N.L., *et al.*, "NASA's New Breakup Model of EVOLVE 4.0," *Adv. Space Res.* 28(9), pp. 1377-84, (2001).
3. Cowardin, H., *et al.*, "Updates to the DebrisSat Project in Support of Improving Breakup Models and Orbital Debris Risk Assessments," ASME, <https://doi.org/10.1115/HVIS2019-066>, (2019).
4. Murray, J., *et al.*, "Analysis of the DebrisSat Fragments and Comparison to the NASA Standard Satellite Breakup Model," First International Orbital Debris Conference, Houston, Texas <https://www.hou.usra.edu/meetings/orbitaldebris2019/orbital2019paper/pdf/6135.pdf> (2019).
5. McKnight, D., *et al.*, "Satellite Orbital Debris Characterization Impact Test (SOCIT) Series Data Collection Report," Kaman Sciences Corporation report, Contract Number NAS 9-19215, (1995). ♦

MEETING REPORT

1st MASTER Workshop 2021, 2-4 March 2021 (Virtual)

The 1st MASTER Workshop 2021, hosted by the European Space Agency (ESA) Space Debris Office, was held virtually 2-4 March 2021. This virtual workshop was developed to initiate the discussion on how collaborative approaches can be established to facilitate exchange of data and measurement collection (including ground-based measurements, in-situ detectors, returned surfaces, and novel measurements), its interpretation and application in the context of ESA's Meteoroid and Space Debris Terrestrial Environment Reference (MASTER) model, the use-cases of the model, and its relevance in mission design. The workshop consisted of daily technical sessions, followed by small-group break-out sessions and a final wrap-up session to review topics discussed during the break-out sessions. Technical sessions included Measurements and Model Validation, Working with MASTER, and A Future Scenario.

The NASA Orbital Debris Program Office presented "Orbital Debris Engineering Model (ORDEM) 3.1 Development and

Validation," providing an overview of the process for building and validating ORDEM from measurement data, and serving as a model comparison to the ESA MASTER model. It is worth noting that the majority of presentations in the Measurements and Model Validation session focused on various types of sensors for collecting measurements of millimeter-sized debris. This reflects the increasing recognition of this size regime as the most critical for operational spacecraft safety in low Earth orbit and highlights the importance of collecting more and improved measurements of the millimeter-sized debris population.

This inaugural workshop lays the foundation for continued collaboration among modelers and model users to improve communication and provide solutions to benefit the entire community. Presentations submitted to the workshop can be downloaded by selecting the "Contribution List" link from the conference website at <https://indico.esa.int/event/370/>. ♦

DAS 3.1 NOTICE

Attention DAS Users: DAS 3.1.1 has been updated to DAS 3.1.2. Previous versions of DAS should no longer be used. NASA regulations require that a Software Usage Agreement must be obtained to acquire DAS 3.1.2. DAS 3.1.2 requires the Windows operating system and has been extensively tested in Windows 10.

To begin the process, click on the Request Now! button in the NASA Software Catalog at <https://software.nasa.gov/software/MSO-26690-1>. Users who have already completed the software request process for earlier versions of DAS 3.x do not need to reapply for DAS 3.1.2. Simply go to your existing account on the NASA Software portal and download the latest installer.

An [updated solar flux table](#) (created 30 March 2021) can be downloaded for use with DAS 3.1.2.

UPCOMING MEETINGS

These events could be canceled or rescheduled due to the COVID-19 pandemic. All information is current at the time of publication. Please consult the respective websites for updated schedule changes.

7-12 August 2021: the 35th Annual Small Satellite Conference-Virtual, Logan, UT, USA

Utah State University (USU) and the AIAA will sponsor the 35th Annual AIAA/USU Conference on Small Satellites, whose theme is “Mission Operations and Autonomy: operations and data delivery at the speed of light,” and will explore the realm of new space mission operations and autonomy enablers. The abstract submission deadline has passed. Conference information is available at the organizer’s website at <https://smallsat.org/>.

14-17 September 2021: 22nd Advanced Maui Optical and Space Surveillance Technologies Conference, Maui, Hawaii, USA

The technical program of the 22nd Advanced Maui Optical and Space Surveillance Technologies Conference (AMOS) will focus on subjects that are mission critical to Space Situational Awareness/Space Domain Awareness. The technical sessions include papers and posters on Orbital Debris, Space Situational/Space Domain Awareness, Adaptive Optics & Imaging, Astrodynamics, Non-resolved Object Characterization, and related topics. The abstract submission deadline has passed. Additional information about the conference is available at <https://amostech.com>.

19-21 October 2021: Hybrid 11th International Association for the Advancement of Space Safety (IAASS) Conference, Osaka, Japan

The 11th conference of the IAASS, organized in concert with the Japan Aerospace Exploration Agency, has as its theme “Managing Risk in Space.” Major debris-related topics include designing safety into space vehicles, space debris mitigation and remediation, re-entry safety, nuclear safety for space missions, safety risk management and probabilistic risk assessment, and launch and in-orbit collision risk. The conference’s abstract submission deadline has passed. Additional information for the 2021 IAASS is available at <http://iaassconference2021.space-safety.org/>.

25-29 October 2021: 72nd International Astronautical Congress (IAC) – Dubai, United Arab Emirates

The IAC will convene with a theme of “Inspire, Innovate & Discover, for the Benefit of Humankind.” The IAC’s 19th IAA Symposium on Space Debris shall cover debris measurements, modeling, risk assessment including re-entry hazards, mitigation and remediation, hypervelocity impact and protection, political and legal aspects of space debris mitigation and removal, and allied subjects. The abstract submission deadline has passed. Additional information for the 2021 IAC is available at <https://www.iaastro.org/events/iac/iac-2021/> and <https://iac2021.org/>.

26 February-4 March 2022: 33rd International Symposium on Space Technology and Science, Beppu, Ōita Prefecture, Japan

The 33rd International Symposium on Space Technology and Science (ISTS) will be conducted jointly with the 10th Nano-Satellite Symposium & 14th International Academy of Astronautics (IAA) Low-Cost Planetary Missions Conference. ISTS will feature a dedicated session on Space Environment and Debris, including modeling, measurements, mitigation and protection, remediation, international cooperation, space weather, space situational awareness, space traffic management, and associated topics. The abstract deadline is 16 August 2021. Additional information about the conference is available at <https://www.ists.or.jp/>.

4-6 April 2022 (tentative): 3rd IAA Conference on Space Situational Awareness, Madrid, Spain

The International Academy of Astronautics (IAA) and the University of Florida will convene the 3rd IAA Conference on Space Situational Awareness in 2022; the University of Florida will provide a remote participation option should the COVID-19 pandemic not be resolved by meeting time. Topics include, but are not limited to, resident space object sensing, identification, association, risk assessment, remediation and reentry, and policy. Abstract submission closes on 15 January 2022. Please see <http://reg.conferences.dce.ufl.edu/ICSSA/1575> or <https://iaospace.org/event/3rd-iaa-conference-on-space-situational-awareness-icssa-2021/> for further information.

